

HETEROCYCLES, Vol. 100, No. 10, 2020, pp. 1686 - 1693. © 2020 The Japan Institute of Heterocyclic Chemistry
Received, 10th July, 2020, Accepted, 6th August, 2020, Published online, 7th August, 2020
DOI: 10.3987/COM-20-14320

UKIXANTHOMYCIN A: A HEXACYCLIC XANTHONE FROM THE MUDFLAT-DERIVED ACTINOMYCETE *STREPTOMYCES* sp.

Yuhei Koyanagi,[†] Teppei Kawahara,[†] Yuki Hitora, and Sachiko Tsukamoto*

Graduate School of Pharmaceutical Sciences, Kumamoto University, Kumamoto 862-0973, Japan; E-mail: sachiko@kumamoto-u.ac.jp

[†] These authors contributed equally to this work.

Abstract – A new hexacyclic xanthone, ukixanthomycin A (**1**), was isolated from the mudflat-derived *Streptomyces* sp. HGMA004 by screening based on chemical analysis by UPLC-HRMS with our in-house actinomycete extract library. The structure of **1** was elucidated by spectral analyses and quantum chemical calculations. Compound **1** showed weak antifungal activity against *Candida albicans*.

Microbial secondary metabolites are known to be a rich source for the discovery of drug leads and biochemical probes due to their chemical diversity and variety of biological activities.^{1,2} Marine and terrestrial microorganisms, particularly actinomycetes, have attracted considerable attention as important resources for new biologically active metabolites.³

The tideland is a submerged or exposed area at the seashore during the rise and fall of the tide, and the intertidal regions are known to harbor unique microbiotas.⁴ So far, structurally intriguing and biologically active metabolites have been obtained from mudflat-derived microorganisms such as buanmycin,⁵ mohangic acids,⁶ WS9326H,⁷ anithiactins,⁸ and hormaomycins⁹ from actinomycetes and oxysporizoline¹⁰ and cristazine¹¹ from fungi.

To discover novel antibiotics from mudflat-derived actinomycetes, we isolated over 400 strains (HGMA strains) from the intertidal mudflat and analyzed their metabolites by a combination of the UPLC-UV/vis-HRMS system and natural products databases,^{12,13} including the Dictionary of Natural Products,¹⁴ SciFinder,¹⁵ and our in-house UPLC/MS data library. In the course of our screening based on chemical analysis, we succeeded in uncovering many novel metabolites in the bacterial extracts. Recently, a new hexacyclic xanthone, ukixanthomycin A (**1**), was isolated from cultured *Streptomyces* sp. HGMA004 along with the known pentacyclic xanthone, buanmycin (**2**) (Figure 1). Compound **1** showed

a characteristic UV spectrum with a longer-wavelength absorption and had a molecular ion peak at m/z 562.1351. We here report the fermentation, isolation, structural elucidation, and biological activities of **1**.

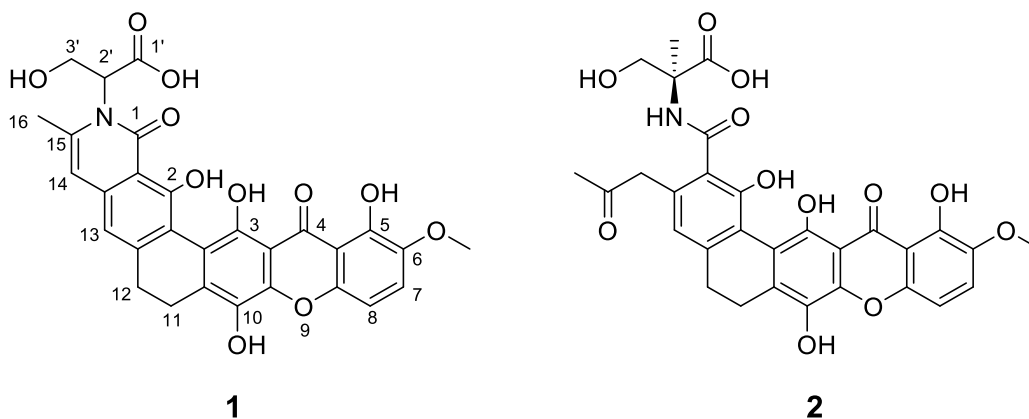


Figure 1. Structures of **1** and **2**

Culture broth of the *Streptomyces* sp. HGMA004 was extracted by EtOAc. A LCMS-guided fractionation of the extract afforded ukixanthomycin A (**1**). The molecular formula of **1** was determined to be $C_{29}H_{23}NO_{11}$ on the basis of HRESI-MS (m/z 562.1351 $[M+H]^+$, calcd for $C_{29}H_{24}NO_{11}$, 562.1349). The IR spectrum showed absorptions corresponding to carbonyl (1648 and 1597 cm^{-1}) and hydroxy (3383 cm^{-1}) groups. The UV absorbances at 260 , 304 , 330 , 356 , 372 , and 438 nm together with 19 degrees of unsaturation indicated the presence of a highly conjugated ring system.

Substructures A–C in **1** were indicated by the analyses of 2D NMR spectra including COSY, HSQC, ^1H – ^{13}C HMBC, and ^1H – ^{15}N HMBC (Figure 2). Because several protons, which were observed as broad signals at $25\text{ }^\circ\text{C}$, became sharp at $100\text{ }^\circ\text{C}$, the 2D spectra were measured at $100\text{ }^\circ\text{C}$ in $\text{DMSO-}d_6$. This indicated that conformational interchange may occur at $25\text{ }^\circ\text{C}$, and made the signals broader. A COSY correlation between $\text{H-2}'$ (δ_{H} 5.03) and $\text{H}_2\text{-3}'$ (δ_{H} 4.17), ^1H – ^{13}C HMBC correlations from $\text{H-2}'$ and $\text{H-3}'$ to $\text{C-1}'$ (δ_{C} 168.7), and a ^1H – ^{15}N HMBC correlation $\text{H-3}'/\text{N-4}'$ (δ_{N} 162.7) showed the presence of *N*-disubstituted serine moiety (Figure 2A) (Table 1). HMBC correlations from $\text{H}_3\text{-16}$ (δ_{H} 2.46) to C-15 (δ_{C} 140.6) and C-14 (δ_{C} 106.8) indicated the presence of a partial structure, $\text{MeC}=\text{CH}$ (Figure 2B). H-14 in turn exhibited correlations to C-1a (δ_{C} 109.0), C-13a (δ_{C} 136.6), and a hydroxylated aromatic carbon C-2 (δ_{C} 157.2, a weak four-bond correlation). The characteristic chemical shifts of C-1 (δ_{C} 165.7) and C-15 (δ_{C} 140.6) together with ^1H – ^{15}N HMBC correlations from $\text{H}_3\text{-16}$ and H-14 to $\text{N-4}'$ indicated the presence of a δ -lactam ring. HMBC correlations were observed from H-13 (δ_{H} 6.91) to C-1a (δ_{C} 109.0), C-2a (δ_{C} 114.3), C-12 (δ_{C} 29.7), and C-14 in addition to weak four-bond correlations to a carbonyl carbon C-1 (δ_{C} 165.7) and C-2b (δ_{C} 113.8). A COSY correlation between $\text{H}_2\text{-11}$ (δ_{H} 2.88) and $\text{H}_2\text{-12}$ (δ_{H} 2.75) together with HMBC correlations from $\text{H}_2\text{-12}$ to C-2a , C-10a (δ_{C} 138.5), and C-12a (δ_{C} 146.6) were

observed. Thus, substructure B was established (Figure 2B). Further, HMBC correlations H-2'/C-1 and H-14, H-16 and H-3'/N-4' revealed the connection of substructures A and B through the nitrogen atom N-4'.

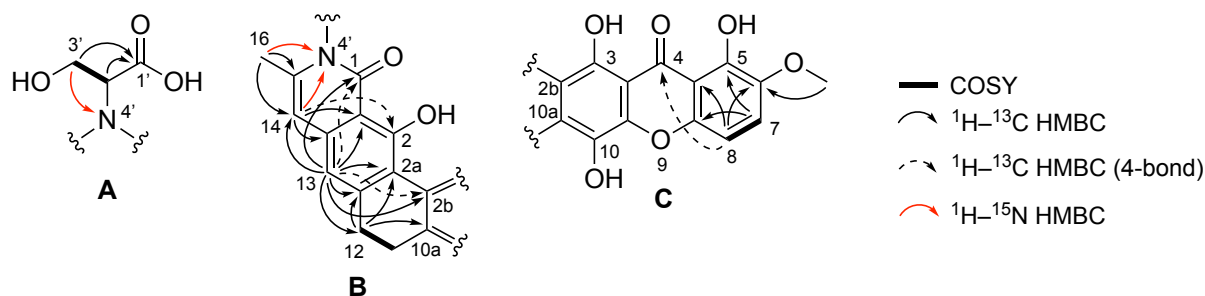


Figure 2. ^1H - ^1H COSY, ^1H - ^{13}C HMBC, and ^1H - ^{15}N HMBC correlations of substructures A–C in **1**

Table 1. ^1H , ^{13}C , and ^{15}N NMR data for **1** in $\text{DMSO-}d_6$ at 100 °C

No.	δ_{C} , type	δ_{H} , mult. (J in Hz)	δ_{N} , type
1	165.7, C		
1a	109.0, C		
2	157.2, C		
2a	114.3, C		
2b	113.8, C		
3	148.9, C		
3a	105.5, C		
4	185.6, C		
4a	107.5, C		
5	149.6, C		
6	142.4, C		
7	122.8, CH	7.56, d (9.1)	
8	106.5, CH	7.07, d (9.1)	
8a	149.3, C		
9a	144.1, C		
10	132.1, C		
10a	138.5, C		
11	23.2, CH_2	2.88, m	
12	29.7, CH_2	2.75, m	
12a	146.6, C		
13	111.7, CH	6.91, s	

13a	136.6, C	
14	106.8, CH	6.54, s
15	140.6, C	
16	20.2, Me	2.46, s
1'	168.7, C	
2'	60.2, CH	5.03, t (6.4)
3'	58.4, CH ₂	4.17, d (6.4)
4'		162.7, N
3-OH		11.81, brs
6-OMe	56.9, Me	3.88, s

The remaining signals in the lowfield region were reminiscent of **2**, indicating **1** to be a xanthone derivative. Two doublet ($J = 9.1$ Hz) aromatic signals H-7 (δ_{H} 7.56) and H-8 (δ_{H} 7.07) indicated the presence of a 1,2,3,4-tetrasubstituted aromatic ring (Figure 2C). HMBC correlations from H-7 to C-5 (δ_{C} 149.6) and C-8a (δ_{C} 149.3) and from H-8 to C-4a (δ_{C} 107.5) and C-6 (δ_{C} 142.4) indicated C-5, C-6, and C-8a to be oxygenated olefins. A HMBC correlation from a methoxy signal (δ_{H} 3.88) to C-6 showed that the methoxy group was attached to this carbon. The remaining four unassigned ^{13}C signals (δ_{C} 105.5, 132.1, 144.1, and 148.9) and a HMBC correlation from H-8 to C-4 (δ_{C} 185.6, weak) indicated the presence of a 1,2,3,4,7,8-hexasubstituted xanthone substructure (Figure 2C). These carbons were likely to be assigned as C-3a (δ_{C} 105.5), C-10 (δ_{C} 132.1), C-9a (δ_{C} 144.1), and C-3 (δ_{C} 148.9), compared with those of **2**.¹⁶

There are two possibilities for the connection of substructures B and C. To determine the gross structure of **1**, the ^{13}C chemical shifts of two simplified models **a** and **b** (Figure 3A), in which the substituent at N-4' was replaced with a hydrogen atom, were calculated by Spartan'18 at the $\omega\text{B97X-D/6-31G}^*$ level (Figure 3B). Model **a** has the same connection as **2** and, in contrast, model **b** has the opposite one. The standard deviations of the differences between experimental and calculated values were 3.0 (model **a**) and 6.2 (model **b**) (Tables S1 and S2). The experimental data better matched the calculated values of model **a** compared to those of model **b**. Among these, the calculated values of C-2b and C-10a of model **b** were significantly different from those of **1**. Therefore, these data established the planar structure of **1**, leaving the absolute configuration of C-2' undetermined.¹⁷ Septacyclic xanthenes, arixanthomycins A–C¹⁸ and citreamicin ϵ ,¹⁹ also possess the same ring system as model **a**.

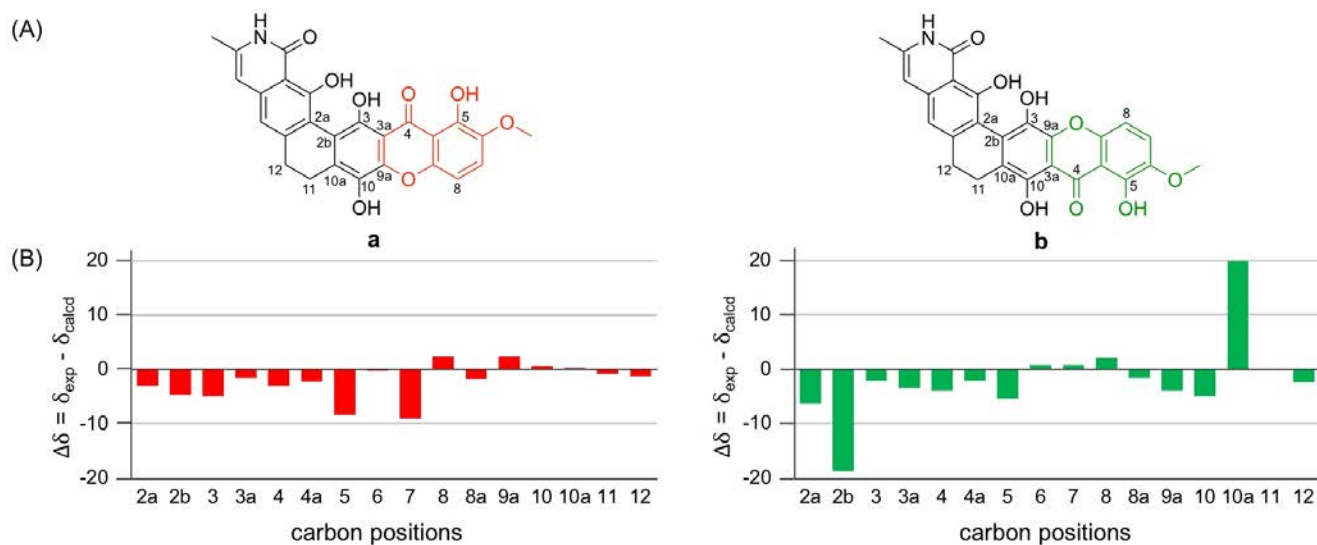


Figure 3. (A) Simplified models **a** and **b** for **1**. (B) Difference of ^{13}C chemical shifts between the experimental and calculated values for **a** and **b**.

BIOLOGICAL ACTIVITIES

Ukixanthomycin A (**1**) showed no cytotoxic activity against A549 and HeLa cells at 200 μM and no/weak antimicrobial activities against *Bacillus cereus*, *Escherichia coli*, and *Candida albicans*, although buanmycin (**2**) was active in these tests (Table 2). These data indicated that the formation of the δ -lactam ring in **1** might reduce these activities.

Table 2. Cytotoxic and antimicrobial activities of **1** and **2**

Compound	IC ₅₀ (μM)		GI ₅₀ (μM)		
	A549	HeLa	<i>B. cereus</i>	<i>E. coli</i>	<i>C. albicans</i>
1	> 200	> 200	> 200	> 200	11.5
2	0.8	0.9	3.0	6.0	0.4

EXPERIMENTAL

General Experimental Procedures.

Optical rotation was measured on a JASCO DIP-1000 polarimeter in MeOH. UV spectrum was measured on a JASCO V-550 spectrophotometer in MeOH. IR spectrum was recorded on a Perkin Elmer Frontier FT-IR spectrophotometer. NMR spectra were measured on a JEOL JNM-ECX400 spectrometer, except for ^1H - ^{15}N NMR spectrum on a Bruker Avance I 600 NMR spectrometer. Chemical shifts were referenced to the residual solvent peaks (δ_{H} 2.49 and δ_{C} 39.5 for DMSO- d_6) or the internal offset for ^{15}N assigned by the instrument manufacturer (Bruker). ESI-HRMS data were recorded on a Waters Xevo

G2-XS QToF mass spectrometer. The preparative MPLC was performed on a Biotage Isolera I. The preparative HPLC system comprised a Waters 515 HPLC pump, Waters 2489 UV/visible detector, and Pantos Unicorder U-228.

Bacterial Strain.

Strain HGMA004 was isolated from a mudflat sediment collected at Uki, Kumamoto Prefecture, Japan, in 2016. The strain was identified as *Streptomyces* sp. according to its 16S rDNA sequence analyzed by TechnoSuruga Laboratory Co., Ltd. Its 463, 461, and 458 base pair 16S rDNA sequences had 100% identity to those of *S. griseoloalbus* NBRC13046 (AB184275), *S. albaduncus* JCM4715 (AY999757), and *S. capillispiralis* NBRC14222 (AB184577), respectively. The sequence data of this strain are deposited to GenBank with accession number MT634708.

Culture Conditions.

The bacterium was cultivated in 500-mL baffled Erlenmeyer flasks, each containing 100 mL of seed medium consisting of 0.3% D-glucose, 0.8% soybean meal, 0.3% yeast extract, and 1.6% artificial sea salt, adjusted to pH 7.5 before sterilization. The flasks were shaken on a rotary shaker (200 rpm) at 27 °C for 2 days. Aliquots (2.5 mL) of the culture were transferred into 500-mL baffled Erlenmeyer flasks filled with 100 mL of a production medium consisting of 4.5% glycerol, 4.5% D-glucose, 1.0% fish meal extract, 0.1% CaCO₃, 1.6% artificial sea salt, and 0.1% Diaion HP-20, adjusted to pH 7.4 before sterilization, and then cultured on a rotary shaker (200 rpm) at 27 °C for 3 days. During the optimization of culture conditions, we found that **1** and **2** were not produced in the freshwater medium, indicating that salt was necessary for their production.

Extraction and Isolation.

The fermentation broth (3 L) was separated into the supernatant and mycelial cake by vacuum filtration. After extraction of the supernatant with EtOAc (1 L × 3), the organic layer was concentrated *in vacuo*. The yellow extract (156.3 mg), which showed the presence of a novel metabolite in LCMS analysis, was subjected to silica gel MPLC (Purif-Pack[®]-EX SI-25μm, SHOKO SCIENCE Co., Ltd., size: 60) eluted with a linear gradient system of 0–15% EtOAc–*n*-hexane and then 0, 1, 2, 5, 10, 30, 50, and 100% MeOH–CH₂Cl₂. The fraction eluted by 10% MeOH–CH₂Cl₂ was subject to reversed-phase MPLC (Purif-Pack[®]-EX ODS-25μm, SHOKO SCIENCE Co., Ltd., size: 60) with 40, 60, 80, and 100% MeOH–H₂O. The fraction eluted by 80% MeOH–H₂O fraction (17.2 mg) was purified by ODS HPLC (COSMOSIL 5C18-MS-II column, Nacalai Tesque Inc., 20 × 250 mm; flow rate, 6 mL/min; detector, UV 254 and 350 nm) with 60% MeOH–H₂O containing 0.2% formic acid to yield **1** (6.0 mg; T_R, 40.5 min) and **2** (4.5 mg; T_R, 24.3 min).

Ukixanthomycin A (1): Yellow powder; $[\alpha]_D^{25} +13$ (*c* 0.2, MeOH); UV (MeOH) λ_{\max} (log ϵ) 242 (4.84), 260 (4.80), 304 (4.56), 330 (4.67), 356 (4.70), 372 (4.68), 438 (3.86) nm; IR (film) ν_{\max} 3383, 2923, 2852,

1648, 1597, 1487, 1275, 1025 cm^{-1} ; ^1H and ^{13}C NMR data, see Table 1; ESI-HRMS m/z 562.1351 $[\text{M} + \text{H}]^+$ (calcd for $\text{C}_{29}\text{H}_{24}\text{NO}_{11}$, 562.1349).

Conformational Analyses and Chemical Shift Calculations for Models a and b.

These experiments were performed as previously described.²⁰ Chemical shift calculations were performed at the $\omega\text{B97X-D/6-31G}^*$ level.

Cytotoxicity and Antimicrobial Assay.

The details of the biological assay performed in this experiment were previously described.^{21,22}

ACKNOWLEDGEMENTS

This work was supported by JSPS KAKENHI Grants 19K07135 (T. K.), 18K14933 (Y. H.), and 20H03396 (S. T.) and Useful and Unique Natural Products for Drug Discovery and Development (UpRoD), Program for Building Regional Innovation Ecosystems at Kumamoto University, Japan.

REFERENCES AND NOTES

1. E. M. Molloy and C. Hertweck, *Curr. Opin. Microbiol.*, 2017, **39**, 121.
2. N. P. Keller, *Nat. Rev. Microbiol.*, 2019, **17**, 167.
3. P. R. Jensen, B. S. Moore, and W. Fenical, *Nat. Prod. Rep.*, 2015, **32**, 738.
4. H. Stevens, T. Brinkhoff, B. Rink, J. Vollmers, and M. Simon, *Environ. Microbiol.*, 2007, **9**, 1810.
5. K. Moon, B. Chung, Y. Shin, A. L. Rheingold, C. E. Moore, S. J. Park, S. Park, S. K. Lee, K. B. Oh, J. Shin, and D. C. Oh, *J. Nat. Prod.*, 2015, **78**, 524.
6. M. Bae, K. Moon, J. Kim, H. J. Park, S. K. Lee, J. Shin, and D. C. Oh, *J. Nat. Prod.*, 2016, **79**, 332.
7. M. Bae, J. Oh, E. S. Bae, J. Oh, J. Hur, Y. G. Suh, S. K. Lee, J. Shin, and D. C. Oh, *Org. Lett.*, 2018, **20**, 1999.
8. H. Kim, I. Yang, R. S. Patil, S. Kang, J. Lee, H. Choi, M. S. Kim, S. J. Nam, and H. Kang, *J. Nat. Prod.*, 2014, **77**, 2716.
9. M. Bae, B. Chung, K. B. Oh, J. Shin, and D. C. Oh, *Mar. Drugs*, 2015, **13**, 5187.
10. V. Nenkrep, K. Yun, and B. W. Son, *J. Antibiot.*, 2016, **69**, 709.
11. K. Yun, T. T. Khong, A. S. Leutou, G. D. Kim, J. Hong, C. H. Lee, and B. W. Son, *Chem. Pharm. Bull.*, 2015, **64**, 59.
12. D. Krug and R. Müller, *Nat. Prod. Rep.*, 2014, **31**, 768.
13. B. C. Covington, J. A. McLean, and B. O. Bachmann, *Nat. Prod. Rep.*, 2017, **34**, 6.
14. <http://dnp.chemnetbase.com/>
15. <https://scifinder.cas.org/scifinder/>
16. The corresponding ^{13}C chemical shifts of **2** were δ_{C} 148.8 (C-3), 144.6 (C-9a), 133.7 (C-10), and 105.9 (C-3a). Although the chemical shift of C-10 of **2** was reported as δ_{C} 138.3,⁵ we found that the

assignment of C-10 and C-10a was reversed.

17. To determine the absolute configuration of C-2', we tried to prepare (*R*)- and (*S*)-PGME amides²³ of **1**, but it was unsuccessful. Further, we tried to hydrolyze **1** to liberate the serine residue, but it was also unsuccessful.
18. H. S. Kang and S. F. Brady, *ACS Chem. Biol.*, 2014, **9**, 1267.
19. D. C. Hopp, D. J. Milanowski, J. Rhea, D. Jacobsen, J. Rabenstein, C. Smith, K. Romari, M. Clarke, L. Francis, M. Irigoyen, M. Luche, G. J. Carr, and U. Mocek, *J. Nat. Prod.*, 2008, **71**, 2032.
20. M. Torii, H. Kato, Y. Hitora, E. D. Angkouw, R. E. P. Mangindaan, N. J. de Voogd, and S. Tsukamoto, *J. Nat. Prod.*, 2017, **80**, 2536.
21. A. H. Afifi, A. H. El-Desoky, H. Kato, R. E. P. Mangindaan, N. J. de Voogd, N. M. Ammar, M. S. Hifnawy, and S. Tsukamoto, *Tetrahedron Lett.*, 2016, **57**, 1285.
22. M. Gushiken, I. Kagiya, H. Kato, T. Kuwana, F. Losung, R. E. P. Mangindaan, N. J. de Voogd, and S. Tsukamoto, *J. Nat. Med.*, 2015, **69**, 595.
23. T. Yabuuchi and T. Kusumi, *J. Org. Chem.*, 2000, **65**, 397.